

# Semi-Analytic Galaxy Formation in coupled Dark Energy Cosmologies

Fabio Fontanot<sup>1\*</sup>, Marco Baldi<sup>2,3,4</sup>, Volker Springel<sup>5,6</sup> and Davide Bianchi<sup>7</sup>

<sup>1</sup> *INAF - Astronomical Observatory of Trieste, via G.B. Tiepolo 11, I-34143 Trieste, Italy*

<sup>2</sup> *Dipartimento di Fisica e Astronomia, Alma Mater Studiorum Università di Bologna, viale Berti Pichat, 6/2, I-40127 Bologna, Italy*

<sup>3</sup> *INAF - Osservatorio Astronomico di Bologna, via Ranzani 1, I-40127 Bologna, Italy*

<sup>4</sup> *INFN - Sezione di Bologna, viale Berti Pichat 6/2, I-40127 Bologna, Italy*

<sup>5</sup> *HITS-Heidelberger Institut für Theoretische Studien, Schloss-Wolfsbrunnengasse 35, 69118 Heidelberg, Germany*

<sup>6</sup> *Zentrum für Astronomie der Universität Heidelberg, ARI, Mönchhofstrasse 12-14, 69120 Heidelberg, Germany*

<sup>7</sup> *Institute of Cosmology and Gravitation, University of Portsmouth, Portsmouth PO1 3FX*

Accepted ... Received ...

## ABSTRACT

Among the possible alternatives to the standard cosmological model ( $\Lambda$ CDM), coupled Dark Energy models postulate that Dark Energy (DE), seen as a dynamical scalar field, may interact with Dark Matter (DM), giving rise to a “fifth-force”, felt by DM particles only. In this paper, we study the impact of these cosmologies on the statistical properties of galaxy populations by combining high-resolution numerical simulations with semi-analytic models (SAM) of galaxy formation and evolution. New features have been implemented in the reference SAM in order to have it run self-consistently and calibrated on these cosmological simulations. They include an appropriate modification of the mass temperature relation and of the baryon fraction in DM haloes, due to the different virial scalings and to the gravitational bias, respectively. Our results show that the predictions of our coupled-DE SAM do not differ significantly from theoretical predictions obtained with standard SAMs applied to a reference  $\Lambda$ CDM simulation, implying that the statistical properties of galaxies provide only a weak probe for these alternative cosmological models. On the other hand, we show that both galaxy bias and the galaxy pairwise velocity distribution are sensitive to coupled DE models: this implies that these probes might be successfully applied to disentangle among quintessence,  $f(R)$ -Gravity and coupled DE models.

**Key words:** galaxies: formation - galaxies: evolution - galaxies: fundamental properties

## 1 INTRODUCTION

Dark Energy (DE) represents a critical unknown for the concordance cosmological model of our Universe, which emerged as the result of a decade long effort in the determination of the key cosmological parameters (see e.g. Planck Collaboration XVI 2014). The easiest description for this mysterious contributor to the present energy density, which accounts for  $\sim 70$  per cent, is a classical cosmological constant  $\Lambda$ , i.e. an homogeneous and static energy density filling the whole Universe at all epochs. This simple model ( $\Lambda$ CDM hereafter), while indeed able to explain the vast majority of the observed properties of the Universe, bears a number of theoretical problems (see e.g. Weinberg 1989, for a review), mostly due to the level of “fine-tuning” required to accommodate for the small value of  $\Lambda$  at the present epoch. A number of alternative DE models have thus been proposed in the literature trying to explain the

origin of the accelerated expansion: these range from scalar field theories (i.e. quintessence), to modifications of the equation of general relativity (see e.g. Amendola 2013, and references therein for a comprehensive review). In order to provide the observational constraints needed to disentangle between those different scenarios, wide galaxy surveys are currently under advanced planning, like the Euclid mission (Laureijs et al. 2011), which relies on a combination of weak lensing measurements (based on precision imaging) and clustering analysis (from slitless spectroscopy), which will allow to study, at the same time, both the evolution of the equation of state of DE and the growth function.

Since galaxies provide the privileged tracers of cosmic evolution, it is crucial, for the success of these missions, to understand the interplay between the physical processes responsible for galaxy formation and evolution and the assembly of the large-scale structure. The former issue has been explored, for a number of alternative cosmologies, with the help of numerical methods that follow the non-linear evolution of virialized structures (i.e. high resolu-

\* E-mail: fontanot@oats.inaf.it

tion  $N$ -body simulations, see e.g. Grossi & Springel 2009; Baldi 2012b; Puchwein et al. 2013 and references herein). In the baryonic sector, semi-analytic models (SAMs) employ simplified analytic prescriptions to model the relevant processes acting on the baryonic gas (and their interplay), and to study the evolution of galaxy components as a function of their physical properties, redshift and environment. This approach has been shown to correctly reproduce a number of observational data, and the predictions of different models are consistent in many cases (Fontanot et al. 2009, 2012), even if some tension with the data still remains (see e.g. McCarthy et al. 2007; Boylan-Kolchin et al. 2012; Weinmann et al. 2012). The analytic prescriptions embedded into SAMs are physically grounded and observationally motivated but involve numerous parameters, which are constrained by requiring the model to reproduce a well defined sample of (typically) low- $z$  observations. This approach thus harbours a significant level of degeneracies (see e.g. Henriques et al. 2009), which are also related to the fact that different authors adopt different approximations for key physical mechanisms. In the context of future space missions, it is therefore of fundamental importance to characterize the impact of alternative DE models on the predicted properties of galaxy populations, in order to devise observational tests that can safely distinguish different cosmological models.

Our group was the first to study the implications of non-standard cosmological scenarios on the relevant properties of galaxies in a large cosmological volume, and to fully quantify their impact on the statistical properties of galaxy populations as predicted by SAMs. We focus on the amplitude of the expected modifications in the galaxy stellar mass function, on the cosmic star formation rate and on the 2-point correlation function, but we also consider higher order statistics like galaxy bias and the galaxy pairwise velocity distribution. For the cosmologies we tested so far, we concluded that galaxy properties alone are usually inefficient to constrain cosmological models beyond  $\Lambda$ CDM, but whenever they are combined with suitable information on the underlying Dark Matter (DM) distribution, it is possible to devise statistical tests able to disentangle these alternative cosmological scenarios from the standard model *and* among themselves. This is the fourth paper on our series: we already considered Early Dark Energy (Fontanot et al. 2012, hereafter Paper I),  $f(R)$ -Gravity (Fontanot et al. 2013, hereafter Paper II) and massive neutrino cosmologies (Fontanot et al. 2015, hereafter Paper III). In this work, we consider a new class of cosmologies, namely the so-called *coupled DE* models (cDE hereafter, see e.g. Wetterich 1995; Amendola 2000), which are based on the dynamical evolution of a classical scalar field  $\phi$  that plays the role of DE, and interacts directly with the Cold Dark Matter (CDM) fluid. As a consequence of the exchange of energy and momentum during cosmic evolution, the DE scalar field thus mediates a “fifth-force” between Dark Matter particles, leading to a modification of the gravitational growth process (both at linear and non-linear scales) and to a different evolution of cosmic large-scale structure.  $N$ -body simulations of cDE cosmologies have been performed by various groups in the last decade (see e.g. Macciò et al. 2004; Baldi et al. 2010; Li & Barrow 2011; Carlesi et al. 2014) and represent now a robust tool to investigate DE interactions in the non-linear regime. The particular imprints of this class of models have been studied in detail by Baldi (2012b) using a suite of  $N$ -body and hydrodynamical simulations (the CoDECS project<sup>1</sup>),

<sup>1</sup> The simulations data of the CoDECS project are publicly available at [www.marcobaldi.it/CoDECS](http://www.marcobaldi.it/CoDECS)

**Table 1.** Cosmological parameters for our simulations. The columns contain from left to right: the normalization  $A$  and the exponent  $\alpha$  of the potential, the strength of the coupling  $\beta$ ,  $\sigma_8$  and the equation of state parameter  $w$  at  $z = 0$ .

	$A$	$\alpha$	$\beta$	$\sigma_8(z = 0)$	$w(z = 0)$
$\Lambda$ CDM	—	—	—	0.809	-1.0
EXP003	0.0218	0.08	0.15	0.967	-0.992
SUGRA003	0.0202	2.15	-0.15	0.806	-0.901

focusing on the degeneracy of DE coupling with other cosmological parameters (like the normalization of the matter power spectrum  $\sigma_8$ ) and on the gravitational bias, i.e. the offset between the density fluctuations in CDM and in the baryonic components (leading to different baryon fraction at cluster scales).

This paper is organized as follows. In Section 2, we introduce the cosmological numerical simulations and semi-analytic models we use in our analysis. We present the predicted galaxy properties and compare them among different cosmologies in Section 3. Finally, we discuss our conclusions in Section 4.

## 2 MODELS

### 2.1 Coupled Dark Energy cosmologies

In this work, we consider a set of flat cosmological models including CDM, baryons, radiation and a DE scalar field  $\phi$ . Among the range of models included in the CoDECS project we focus on two different choices for the scalar field potential. We first consider an exponential potential (Wetterich 1988, the EXP003 model in Baldi 2012b)

$$V(\phi) = A\phi e^{-\alpha\phi}, \quad (1)$$

which is characterized by stable scaling solutions for the scalar field independently from initial conditions. In particular, in cDE scenarios, such a potential provides a transient early DE solution and a late time accelerated attractor (see e.g. Amendola 2004). We also consider a SUGRA potential (Brax & Martin 1999, the SUGRA003 model in Baldi 2012b)

$$V(\phi) = A\phi^{-\alpha} e^{-\phi^2/2} \quad (2)$$

which is typical of supersymmetric theories of gravity and implies a “bounce” of the DE equation of state  $w$  at the cosmological “barrier”  $w = -1$  (see e.g. Baldi 2012a). This feature has relevant implications for the expected number density evolution of DM haloes, as well as for the evolution of the cosmological Hubble function and growth factor (see Baldi 2012b, for more details).

The evolution of the main cosmological components is described by a set of dynamical equations including the interaction between the scalar field and CDM particles (i.e. the right-hand side of Equations 3 and 4):

$$\ddot{\phi} + 3H\dot{\phi} + \frac{dV}{d\phi} = \sqrt{\frac{16\pi G}{3}}\beta(\phi)\rho_c \quad (3)$$

$$\dot{\rho}_c + 3H\rho_c = -\sqrt{\frac{16\pi G}{3}}\beta(\phi)\rho_c\dot{\phi} \quad (4)$$

where  $\rho_c$  represents the density of CDM particles and an overdot denotes the (cosmic) time derivative. In the cDE models considered in this work, the coupling function  $\beta(\phi)$ , which controls the

interaction strength<sup>2</sup>, is assumed to be constant. As baryons and radiations are always uncoupled from  $\phi$  their evolution follows the usual relations  $\rho_b \propto a^{-3}$  and  $\rho_r \propto a^{-4}$ , respectively.

At the level of linear perturbations, the interaction determines a modification of the growth rate due to the presence of a fifth-force with a strength  $4\beta^2/3$  times the standard gravitational acceleration acting between CDM particles, and to an additional velocity-dependent acceleration proportional to  $\dot{\phi}\beta$ . These effective modifications of the standard gravitational evolution affect also the non-linear dynamics of collapsed structures. For a more detailed discussion on the linear and non-linear properties of cDE cosmologies, we refer the reader to Amendola (2004), Baldi et al. (2010) and Baldi (2011).

## 2.2 Numerical simulations

In this work, we take advantage of the results of the CoDECS numerical simulations (Baldi 2012b), using a modified version of the GADGET code (Springel et al. 2005), designed to include the specific physical processes arising in the cDE scenario (Baldi et al. 2010). In particular, we analyse the outcome of the H-CoDECS set, i.e. adiabatic hydrodynamical simulations on periodic boxes  $80 h^{-1} \text{Mpc}$  on a side, using  $2 \times 512^3$  particles (corresponding to a mass resolution of  $2.39 \times 10^8 h^{-1} M_\odot$  for CDM and  $4.78 \times 10^7 h^{-1} M_\odot$  for baryons). An entropy-conserving formulation of smoothed particle hydrodynamics (Springel & Hernquist 2002, SPH) has been used to estimate hydrodynamical forces acting on gas particles, and no additional radiative processes (gas cooling, star formation, feedbacks) have been included. Initial conditions for all runs were generated using N-GENIC by displacing particles from a homogeneous *glass* distribution imposing the same amplitude of the initial power spectrum at the last scattering surface, the same phases and mode amplitudes, to ensure a similar realisation of the large scale structure and to allow an object-by-object comparison. For all simulations, a flat cosmological model has been assumed with  $z = 0$  cosmological parameters consistent with the 7th year results of the *Wilkinson Microwave Anisotropy Probe* (Komatsu et al. 2011, WMAP7), i.e. density parameters  $\Omega_{\text{CDM}} = 0.226$ ,  $\Omega_{\text{DE}} = 0.729$  and  $\Omega_{\text{bar}} = 0.0451$  (for CDM, DE and baryons respectively), Hubble parameter  $h = 0.703$  and Gaussian density fluctuations with a scale-invariant primordial power spectrum with spectral index  $n = 0.966$ . The common normalisation of perturbations at CMB and the different growth factors for cDE runs imply that the EXP003 run has a different amplitude of density perturbation at every redshift and a different  $\sigma_8$  at  $z = 0$ , as listed in Table 1. On the other hand, the SUGRA003 run has, by construction, the same linear normalisation as  $\Lambda\text{CDM}$  both at CMB and at present, with the final results that its  $\sigma_8$  value is very similar to the  $\Lambda\text{CDM}$  run.

For each run, 69 snapshots were stored<sup>3</sup>; the corresponding group catalogues were generated using a Friend-of-Friend algorithm with a linking length of 0.2 (in mean particle separation

<sup>2</sup> In particular, the sign of  $\dot{\phi}\beta(\phi)$  is related to the energy-momentum flow between the two components, such as negative (positive) values of this quantity correspond to a transfer from DE to CDM (from CDM to DE) and to an increase (decrease) of the DM particle mass.

<sup>3</sup> At variance with our previous work, the snapshot list is not the same as in the Millennium simulation; the CoDECS redshift sampling was chosen mostly to allow the construction of full light-cones for weak lensing and CMB lensing purposes (see e.g. Giocoli et al. 2015, and references herein)

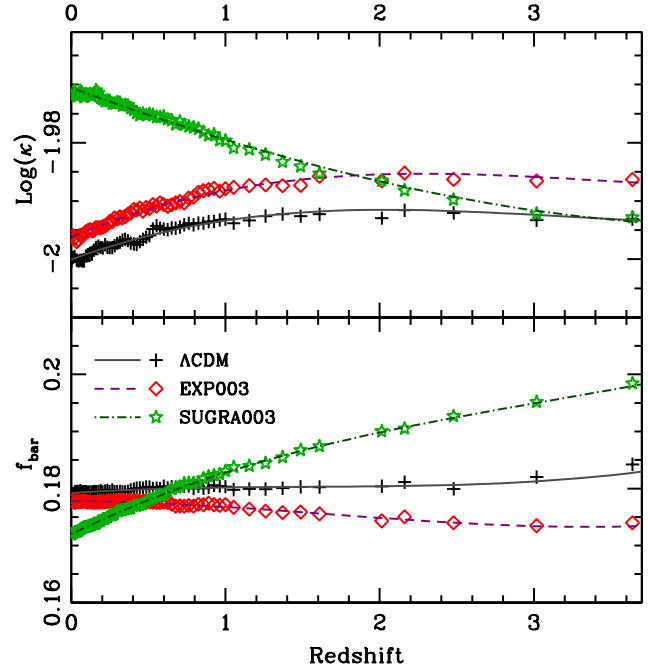


**Figure 1.** Redshift evolution of the normalization of the virial scaling relations for DM haloes ( $\kappa$ , upper panel) and baryon fractions ( $f_{\text{bar}}$ , lower panel). In each panel the black crosses, red diamonds and green stars refer to the  $\Lambda\text{CDM}$ , EXP003 and SUGRA003 runs respectively. Solid, dashed and dot-dashed lines represent the 3-rd order polynomial best fits for each cosmology as indicated in the legends.

units), and gravitationally bound substructures have been identified using SUBFIND (Springel et al. 2001) (only subhaloes that retain at least 20 particles after the gravitational unbinding procedure were considered). We then used the subhalo catalogues to define the merger tree histories as in Springel et al. (2005).

## 2.3 Semi-Analytic Models

In this paper, we consider the same SAM suite we used in the previous papers of the series. This includes three different versions of the L-GALAXIES semi-analytic model, namely those presented in Croton et al. (2006), De Lucia & Blaizot (2007) and Guo et al. (2011). All these models were run by construction on Millennium-like merger trees<sup>4</sup> as defined in the previous section and they represent a coherent set of models<sup>5</sup>, suitable to study the intra-model variance due to different assumptions made in the modelling of the key physical processes. The free parameters usually associated with this approach have been calibrated (for a  $\Lambda\text{CDM}$  cosmological model), by comparing model predictions to a well defined set of observational constraints (mainly at low-redshift). In order to highlight the differences in galaxy properties due to the different

<sup>4</sup> Thus avoiding any additional noise in the predictions due to different definitions of DM merger trees (Knebe & et al. 2015).

<sup>5</sup> These three models mark the historical evolution of the code originally developed by Springel et al. (2005): from Croton et al. (2006) to De Lucia & Blaizot (2007) the main changes involve the treatment of dynamical friction and merger times, the initial mass function (from Salpeter to Chabrier) and the dust modelling; while from De Lucia & Blaizot (2007) to Guo et al. (2011) the modelling of supernovae feedback, the treatment of satellite galaxy evolution, tidal stripping and mergers were added.

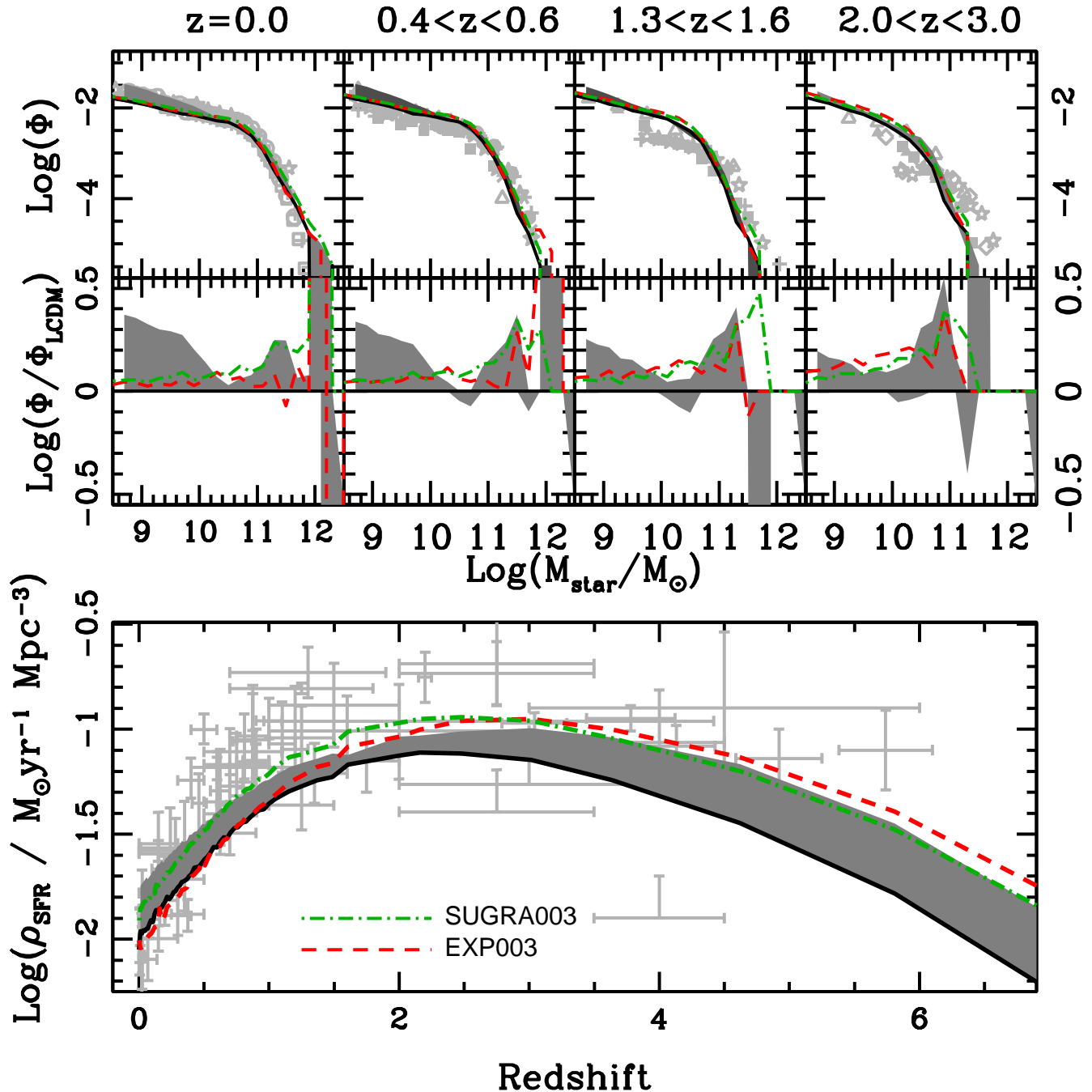


**Figure 2.** Predicted galaxy properties for different coupled Dark Energy cosmological scenarios. *Upper panels:* redshift evolution of the stellar mass function (light grey points refer to the compilation from Fontanot et al. (2009)). The lower row shows the ratio between the mass function in a given cosmological model and the corresponding mass function from the Guo et al. (2011) model in the  $\Lambda$ CDM run. *Lower panel:* Cosmic star formation rate density (light grey points refer to the compilation from Hopkins (2004)). In each panel the solid black, dashed red and dot-dashed green lines refer to SAM predictions in  $\Lambda$ CDM, EXP003 and SUGRA003 cosmologies respectively. Dark grey areas mark the distribution of the predictions from the Guo et al. (2011), De Lucia & Blaizot (2007) and Croton et al. (2006) SAMs applied to the same  $\Lambda$ CDM run.

underlying cosmology, we choose not to recalibrate the models, thus holding the role of other astrophysical processes fixed. This implies that the models are optimally calibrated to reproduce observations only for the  $\Lambda$ CDM run, where we expect the scatter in their predictions to be representative.

In the next section, we present the predictions obtained from

a modified version of the Guo et al. (2011) model<sup>6</sup> run on the cDE boxes. The main changes with respect to the  $\Lambda$ CDM SAM version include the following new features. First, the code handles a

<sup>6</sup> For the sake of simplicity, in the following, we still refer to our modified code as the Guo et al. (2011) model

user-generated Hubble function (tabulated in an external file) extracted from the corresponding numerical realization of the cDE cosmology under analysis. In Paper II, we showed that, for cosmologies introducing a fifth force, the virial scaling relations deviate from the  $\Lambda$ CDM expectations (see also Arnold et al. 2014), i.e. the relation between total DM mass inside a sphere with interior mean density 200 times the critical density at a given redshift and the one-dimensional velocity dispersion inside the same radius<sup>7</sup> is modified. As in Paper II, we find that the actual relations in cDE cosmologies (defined using  $> 10^{12} M_{\odot}$  DM haloes) are offset versions of  $\Lambda$ CDM ones (see e.g. Fig. 1 in Paper II). Nonetheless, at variance with the constant shift for unscreened haloes we found in the  $f(R)$ -Gravity case, the offset for cDE cosmologies is redshift dependent, and smaller in amplitude (roughly corresponding to a 1 percent variation at most). We show the different values for the normalization  $\kappa$  of the fitted virial relations in Fig. 1 (upper panel). As in Paper II, we then apply a correction to the virial scalings assumed in L-GALAXIES, corresponding to the ratio between the virial scalings in the desired cosmology and the corresponding virial scalings in the  $\Lambda$ CDM run with the same initial conditions. We then model the evolution of the offsets as a 3-rd order polynomial as a function of redshift.

A specific feature of cDE cosmologies is the different baryon fraction ( $f_{\text{bar}}$ ) (Baldi et al. 2010) in massive haloes, due to the different forces felt by the baryons and DM particles. We estimate  $f_{\text{bar}}$  for  $> 10^{12} M_{\odot}$  DM haloes in our simulations and show the redshift evolution of this quantity in Fig. 1 (bottom panel). Our results confirm the Baldi et al. (2010) results; we also stress that  $f_{\text{bar}}$  evolves as a function of redshift, and it does not show any DM mass dependence at fixed cosmic epoch. Typical differences with respect to the  $\Lambda$ CDM run are smaller than 3 percent at  $z < 2$ . In L-GALAXIES,  $f_{\text{bar}}$  mainly regulates the infall of pristine gas when DM haloes grow by accretion from the surrounding field and it is usually treated as a redshift independent free parameter. In our modified code, we still keep the baryon fraction as a free parameter, but we require it to scale, at a given redshift, as the ratio between the corresponding  $f_{\text{bar}}$  in the cDE and  $\Lambda$ CDM boxes. Also in this case, we model the baryon fraction evolution in different cosmologies as a 3-rd order polynomial in redshift. It is worth stressing, that the  $f_{\text{bar}}$  shown in Fig. 1 refers to the ratio between the mass in baryons and the DM mass, yielding a definition closer to the quantities actually used in L-GALAXIES. We also consider the alternative definition of  $f_{\text{bar}}$  as the ratio between the baryonic mass and the total mass in the halo: for all cosmological models, the different definition mainly changes the normalization of  $f_{\text{bar}}(z)$ , but not its evolution. Therefore, as our modifications to L-GALAXIES involve only fractional quantities, our results are insensitive to the  $f_{\text{bar}}$  definition employed.

It is also worth stressing that these two features we included in the SAM have a limited (but not negligible) impact on model predictions, due to the small offsets with respect to the  $\Lambda$ CDM realization and that most of the differences we will discuss in the following are triggered by differences in merger trees and cosmic growth history of the large scale structure realized in the cosmological volumes under analysis.

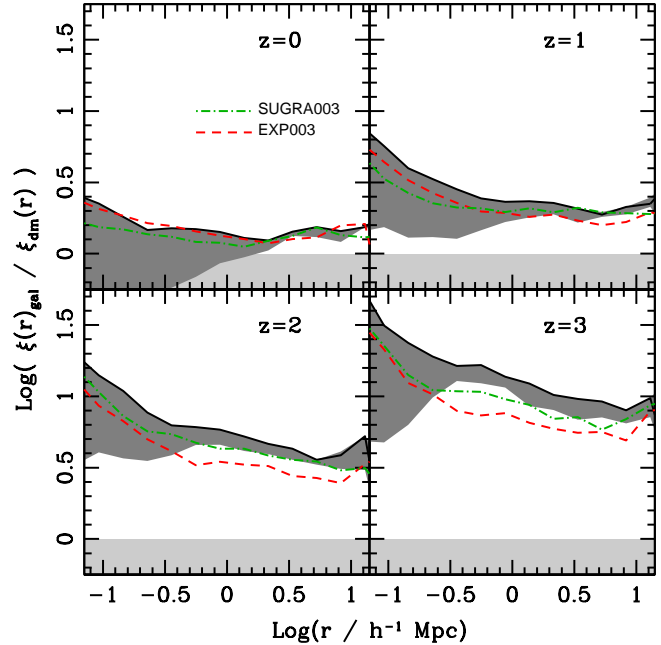


**Figure 3.** Redshift evolution of galaxy bias. In each panel, only model galaxies with  $M_{\star} > 10^9 M_{\odot}$  have been considered. Line types, colours and shaded areas have the same meaning as in Figure 2.

### 3 RESULTS & DISCUSSION

In Figure 2, we present a selection of the statistical properties of  $M_{\star} > 10^9 M_{\odot}$  galaxies, as predicted by the different SAMs. In the upper and lower panels, we show the redshift evolution of the galaxy stellar mass function and cosmic star formation rate, respectively. The model predictions have been convolved with a lognormal error distribution with amplitude 0.25 (0.3) for stellar masses (star formation rates) to account for the typical observational error in the estimate of these physical quantities (Fontanot et al. 2009). Stellar masses and star formation rates in the Croton et al. (2006) model have been converted from Salpeter to Chabrier IMF applying a constant shift of 0.25 and 0.176 dex, respectively. In all panels, solid black lines refer to the predictions of the Guo et al. (2011) model for the  $\Lambda$ CDM simulation. We also consider the predictions of the other two SAMs applied to the same simulation to estimate the scatter in the predictions of different SAMs applied to the same cosmological box (shaded areas): we stress again that the main source of this scatter lies in the different treatment of the key physical mechanisms driving galaxy evolution in the three models. In all panels, we also show the predictions for the modified Guo et al. (2011) model in the EXP003 and SUGRA003 runs, with red dashed and green dot-dashed lines, respectively. As far as galaxy properties are concerned, the deviations of the model predictions in these alternative cosmological scenarios with respect to the reference  $\Lambda$ CDM run are quite small and comparable to the intra-model variance at fixed  $\Lambda$ CDM cosmology. This provides an *a-posteriori* justification for our choice not to recalibrate the model parameters, as the properties of the overall galaxy populations are consistent among the different cosmological runs. There is a slight

<sup>7</sup> Evrard et al. (2008) showed that haloes in  $\Lambda$ CDM cosmology are expected to follow the theoretical scaling  $\sigma_{200} \propto [h(z)M_{200}(z)]^{1/3}$ .

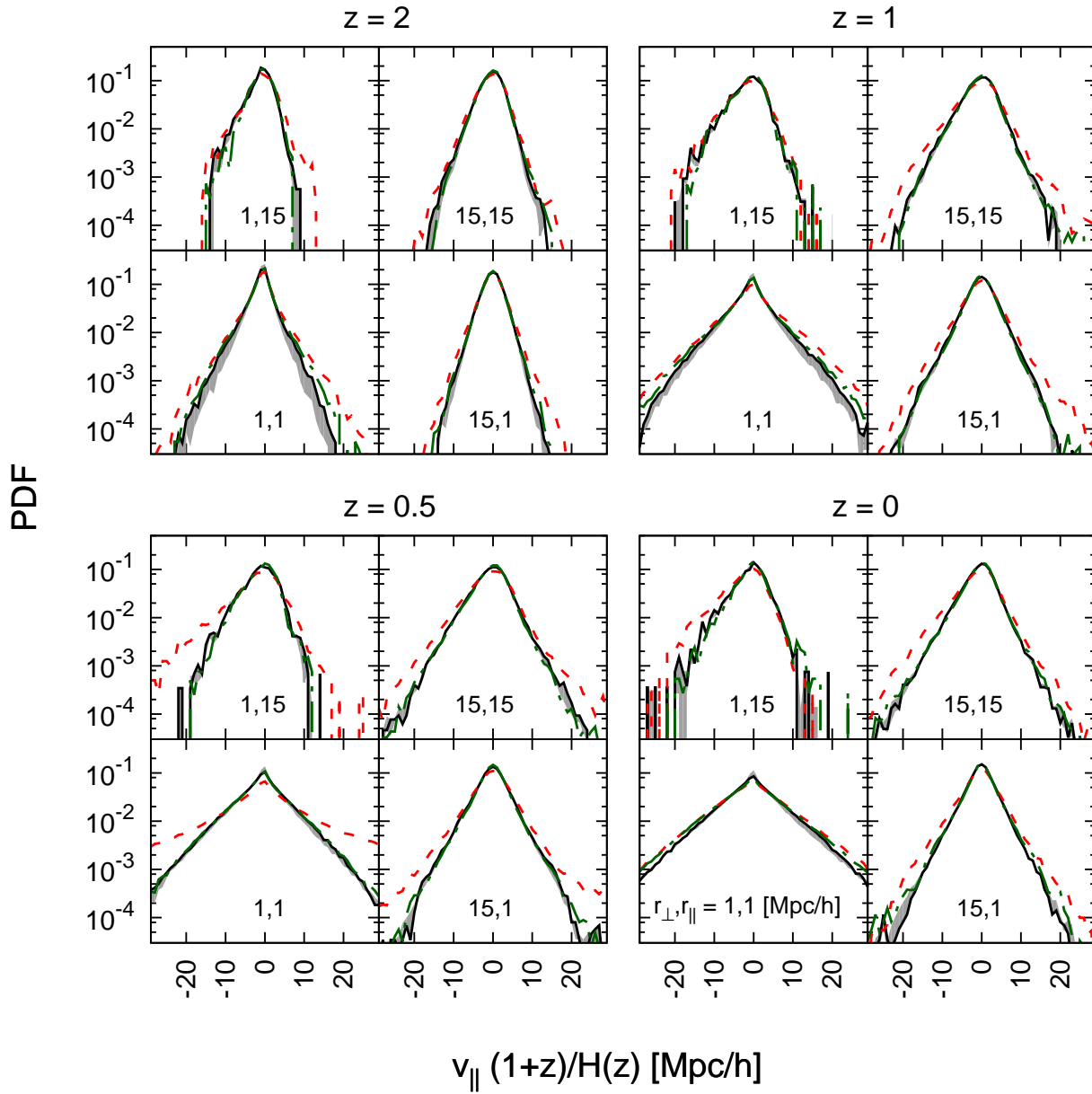


**Figure 4.** Pairwise galaxy velocity distribution along the line of sight for the cDE cosmologies considered in this paper at four different redshifts. Different cosmological models are marked by different linetypes, shading and colours as in Figure 2. The upper left caption in each panel states the different combination for values of the galaxy separation  $(r_{\perp}, r_{\parallel})$ , perpendicular and parallel to the line of sight, respectively; in all panels, the conformal Hubble function  $\mathcal{H} = aH$  has been used to rescale velocities to comoving distances.

tendency for the deviations to grow with redshift, due to the different  $\sigma_8$  value at  $z = 0$ . At variance with the  $f(R)$ -Gravity cosmology we studied in Paper II, we find no relevant dependence of these deviations on stellar mass. In Paper II, we interpret this effect as being due to the different virial scalings in the  $f(R)$ -Gravity model, which directly affect the modeling of AGN feedback. Here the deviations from the  $\Lambda$ CDM virial scalings are definitely smaller than in the  $f(R)$ -Gravity case, and the lack of a stellar mass dependence in the ratio between the mass function in a given cosmology and in

the  $\Lambda$ CDM run, clearly supports our conclusion that this effect is negligible for the cDE cosmologies we consider in this paper. All the differences seen in Fig. 2 are driven by the different merger trees statistics associated with the different cosmologies. Overall, the deviations from the  $\Lambda$ CDM mass function remain within 0.2 dex at most mass scales and redshifts.

In our previous work, we considered two additional cosmological tests, namely galaxy bias and the pairwise velocity distribution, and we discussed their efficiency in disentangling between  $\Lambda$ CDM

and other cosmological scenarios. The discriminating power of these observables is mainly driven by the combination of galaxy populations statistics with information on the distribution of the DM in the underlying large scale structure. In Figure 3, we show the galaxy bias estimates for the cosmological models considered in this work based on the ratio between the auto-correlation function of galaxies in real space  $\xi_{\text{gal}}$  and the corresponding  $\xi_{\text{cdm}}$  computed for a randomly selected subsample of 1 percent of the CDM particles in the cosmological box. Only the EXP003 model shows a deviation from the  $\Lambda$ CDM model larger than the SAM variance in the standard cosmology: in particular this holds at  $z > 1$  and for scales larger than  $\sim 1 h^{-1} \text{Mpc}$ . The different  $\sigma_8$  in the EXP003 run contributes to this deviation, but it cannot totally account for it at scales smaller than  $\sim 10 h^{-1} \text{Mpc}$  and for  $z > 1$ , as shown by Baldi (2012b, their Figure 5). Also the SUGRA003 model shows clear deviations from the corresponding  $\Lambda$ CDM run, but those are of the same order as the intra-SAM variance, thus limiting the efficiency of this estimator in breaking the degeneracies between different cosmologies.

Moreover, in Figure 4 we present the redshift evolution for the pairwise galaxy velocity distribution along the line of sight  $\mathcal{P}(v_{\parallel}, r_{\parallel}, r_{\perp})$ , where we consider fixed components of galaxy separation parallel ( $r_{\parallel}$ ) and perpendicular ( $r_{\perp}$ ) to the line of sight (Scoccimarro 2004, see e.g.). This quantity is a reliable indicator of the assembly of the large scale structure, as it traces the anisotropy of redshift-space correlation functions and it is strongly sensitive to the abundance of massive haloes. In Figure 4 we adopt the same reference separations we choose in our previous work (i.e. 1 and 15  $h^{-1} \text{Mpc}$ ), despite the smaller box size of the H-CODECS runs (i.e. cubic boxes with 80  $h^{-1} \text{Mpc}$  sides). Also in this plot, only galaxies with  $M_{\star} > 10^9 M_{\odot}$  have been considered; furthermore, the velocities have been rescaled using the conformal Hubble function  $\mathcal{H} = aH$  in order for the distribution to represent the statistical displacement of galaxy pairs from real to redshift space. We assume the usual convention that the pairwise velocity is positive when galaxies are receding and negative when they are approaching. This analysis leads us to similar conclusions with respect to Figure 3: the EXP003 model clearly show a different velocity distribution with respect to predictions in the  $\Lambda$ CDM run (due in part, but not completely, to the increase in  $\sigma_8$ ), while the SUGRA003 results are virtually indistinguishable from those obtained for the standard cosmology.

## 4 CONCLUSIONS

In this paper, we present an updated version of the L-GALAXIES semi-analytic model, designed to run self-consistently on the CODECS suite of numerical simulation for coupled Dark Energy cosmologies (Baldi 2012b). The main modifications with respect to the  $\Lambda$ CDM version of the code include: (a) an implementation of an user-defined Hubble function; (b) modified DM halo virial scalings (which impact the mass-temperature relation); (c) modified baryon fractions accounting for the gravitational bias. Item (a) was already introduced in Paper II; item (b) has been modified for this project by allowing a redshift dependence for the virial scaling normalization (with respect to the  $\Lambda$ CDM expectations); item (c) has been introduced in this work. All these new features of the model have been directly calibrated on the cDE simulations under consideration, by comparison with the corresponding  $\Lambda$ CDM runs.

The new code represents a step forward with respect to previous versions, designed to run on Early Dark Energy (Paper I)

and  $f(R)$ -Gravity cosmologies (Paper II), allowing us to present the first comprehensive picture of the impact signature of non-standard coupled-DE cosmologies on the statistical properties of galaxy populations. The weak cosmological constraints coming from direct comparison with model galaxy properties (alone) confirm the robustness of the SAM predictions against small variations in the cosmological framework (see also Wang et al. 2008; Guo et al. 2011). On the other hand, the modification of the cosmological framework we consider has a substantial impact on the growth and assembly of the large scale structure: therefore, combining predicted galaxy properties with information on the distribution of the underlying total mass distribution, it becomes possible to disentangle different cosmological scenarios. In particular, we focus on standard tests like galaxy bias and the galaxy pairwise velocity distribution, and we show that coupled DE models can be distinguished from  $\Lambda$ CDM runs using *both* probes, unlike quintessence models (in Paper I we showed that only bias is a sensitive probe) and  $f(R)$ -Gravity models (in Paper II we showed that only the pairwise velocity distribution is a sensitive probe). However, our results also show that these cosmological tests are sufficiently sensitive only for a subset of coupled DE cosmologies, in particular for the exponential potential run<sup>8</sup>, while the run including a supersymmetric potential corresponds to a much weaker (although coherent) signal. Moreover, in Paper III we showed that the likely existence of a massive neutrino background implies deviations from a pure  $\Lambda$ CDM run which go on in the opposite direction with respect to these results, i.e. an increased galaxy bias and a narrower pairwise distribution. Therefore, the inclusion of such a background would have the net effect of reducing the cosmological signal coming from either coupled DE or  $f(R)$ -Gravity models (as seen i.e. in Baldi et al. 2014).

Overall, the results we presented in our series of papers are of particular relevance for the planning and exploitation of future wide area galaxy surveys (like Euclid, Laureijs et al. 2011), meant to shed light on the true nature of DE. In fact, the wealth of data coming from these efforts requires careful calibration and analysis in order to provide a proper characterization of the large scale structure evolution. Of course, a deep understanding of all the systematic effects, either due to galaxy formation physics or the cosmological parameters, is of critical importance, given the exquisite precision required for disentangling the different scenarios. Therefore, the construction of mock galaxy catalogues covering the widest range of proposed DE theories represents a key step. Our SAM suite, designed to run self-consistently on a variety of these DE models, covers this need and provides a tool to test the relative efficiency of cosmological probes. In this paper, as in our previous work, we focus on scales suitable for galaxy studies (i.e. stellar masses  $10^9 M_{\odot} < M_{\text{star}} < 10^{12} M_{\odot}$ ), but using a moderate volume: we thus plan to apply our SAMs to larger cosmological volumes in the future and use these runs to build cosmological light cones (see e.g. Merson et al. 2013) and mock galaxy catalogues resembling, as close as possible the expected galaxy properties in the different DE cosmologies.

<sup>8</sup> It is worth stressing that the particular model tested in this paper (EXP003) has a relatively strong value of coupling, excluded at about  $3\sigma$  C.L. by the most recent CMB constrains. However, such large coupling values might be still viable in the presence of a substantial (but still reasonable) contribution of massive neutrinos to the cosmic budget.

**ACKNOWLEDGEMENTS**

FF acknowledges financial support from the grants PRIN MIUR 2009 “The Intergalactic Medium as a probe of the growth of cosmic structures” and PRIN INAF 2010 “From the dawn of galaxy formation”. VS acknowledges financial support from the Klaus Tschira Foundation and the Deutsche Forschungsgemeinschaft through Transregio 33, “The Dark Universe”. During the development of this work MB has been partly supported by the Marie Curie Intra European Fellowship “SIDUN” within the 7th Framework Programme of the European Commission. The numerical simulations presented in this work have been performed on the VIP and on the Hydra clusters at the RZG supercomputing centre in Garching.

**REFERENCES**

- Amendola L., 2000, MNRAS, 312, 521  
 Amendola L., 2004, Phys. Rev. D, 69, 103524  
 Amendola L. e. a., 2013, Living Reviews in Relativity, 16, 6  
 Arnold C., Puchwein E., Springel V., 2014, MNRAS, 440, 833  
 Baldi M., 2011, MNRAS, 414, 116  
 Baldi M., 2012a, MNRAS, 420, 430  
 Baldi M., 2012b, MNRAS, 422, 1028  
 Baldi M., Pettorino V., Robbers G., Springel V., 2010, MNRAS, 403, 1684  
 Baldi M., Villaescusa-Navarro F., Viel M., Puchwein E., Springel V., Moscardini L., 2014, MNRAS, 440, 75  
 Boylan-Kolchin M., Bullock J. S., Kaplinghat M., 2012, MNRAS, 422, 1203  
 Brax P. H., Martin J., 1999, Physics Letters B, 468, 40  
 Carlesi E., Knebe A., Lewis G. F., Wales S. and Yepes G., 2014, MNRAS, 439, 2943  
 Croton D. J., Springel V., White S. D. M., De Lucia G., Frenk C. S., Gao L., Jenkins A., Kauffmann G., Navarro J. F., Yoshida N., 2006, MNRAS, 365, 11  
 De Lucia G., Blaizot J., 2007, MNRAS, 375, 2  
 Evrard A. E., Bialek J., Busha M., White M., Habib S., Heitmann K., Warren M., Rasia E., Tormen G., Moscardini L., Power C., Jenkins A. R., Gao L., Frenk C. S., Springel V., White S. D. M., Diemand J., 2008, ApJ, 672, 122  
 Fontanot F., Cristiani S., Santini P., Fontana A., Grazian A., Somerville R. S., 2012, MNRAS, 421, 241  
 Fontanot F., De Lucia G., Monaco P., Somerville R. S., Santini P., 2009, MNRAS, 397, 1776  
 Fontanot F., Puchwein E., Springel V., Bianchi D., 2013, MNRAS, 436, 2672  
 Fontanot F., Springel V., Angulo R. E., Henriques B., 2012, MNRAS, 426, 2335  
 Fontanot F., Villaescusa-Navarro F., Bianchi D., Viel M., 2015, MNRAS, 447, 3361  
 Giocoli C., Metcalf R. B., Baldi M., Meneghetti M., Moscardini L., Petkova M., 2015, ArXiv e-prints (arXiv:1502.03442)  
 Grossi M., Springel V., 2009, MNRAS, 394, 1559  
 Guo Q., White S., Boylan-Kolchin M., De Lucia G., Kauffmann G., Lemson G., Li C., Springel V., Weinmann S., 2011, MNRAS, 413, 101  
 Henriques B. M. B., Thomas P. A., Oliver S., Roseboom I., 2009, MNRAS, 396, 535  
 Hopkins A. M., 2004, ApJ, 615, 209  
 Knebe A., et al. 2015, in preparation  
 Komatsu E., Smith K. M., Dunkley J., Bennett C. L., Gold B., et al., 2011, ApJS, 192, 18  
 Laureijs R., Amiaux J., Arduini S., Auguères J., Brinchmann J., Cole R., Cropper M., Dabin C., Duvet L., Ealet A., et al. 2011, ArXiv e-prints (arXiv:1110.3193)  
 Li B., Barrow J. D., 2011, Phys. Rev. D, 83, 024007  
 Macciò A. V., Quercellini C., Mainini R., Amendola L., Bonometto S. A., 2004, Phys. Rev. D, 69, 123516  
 McCarthy I. G., Bower R. G., Balogh M. L., 2007, MNRAS, 377, 1457  
 Merson A. I., Baugh C. M., Helly J. C., Gonzalez-Perez V., Cole S., Bielby R., Norberg P., Frenk C. S., Benson A. J., Bower R. G., Lacey C. G., Lagos C. d. P., 2013, MNRAS, 429, 556  
 Planck Collaboration XVI 2014, A&A, 571, A16  
 Puchwein E., Baldi M., Springel V., 2013, MNRAS, 436, 348  
 Scoccimarro R., 2004, Phys. Rev. D, 70, 083007  
 Springel V., Hernquist L., 2002, MNRAS, 333, 649  
 Springel V., White S. D. M., Jenkins A., Frenk C. S., Yoshida N., Gao L., Navarro J., Thacker R., Croton D., Helly J., Peacock J. A., Cole S., Thomas P., Couchman H., Evrard A., Colberg J., Pearce F., 2005, Nature, 435, 629  
 Springel V., White S. D. M., Tormen G., Kauffmann G., 2001, MNRAS, 328, 726  
 Wang J., De Lucia G., Kitzbichler M. G., White S. D. M., 2008, MNRAS, 384, 1301  
 Weinberg S., 1989, Reviews of Modern Physics, 61, 1  
 Weinmann S. M., Pasquali A., Oppenheimer B. D., Finlator K., Mendel J. T., Crain R. A., Macciò A. V., 2012, MNRAS, 426, 2797  
 Wetterich C., 1988, Nuclear Physics B, 302, 668  
 Wetterich C., 1995, A&A, 301, 321